When Mamba Meets xLSTM: An Efficient and Precise Method with the XLSTM-VMUNet Model for Skin lesion Segmentation

Zhuoyi Fang   Kexuan Shi   Qiang Han

Yangzhou University

Abstract

Automatic melanoma segmentation is essential for early skin cancer detection, yet challenges arise from the heterogeneity of melanoma, as well as interfering factors like blurred boundaries, low contrast, and imaging artifacts. While numerous algorithms have been developed to address these issues, previous approaches have often overlooked the need to jointly capture spatial and sequential features within dermatological images. This limitation hampers segmentation accuracy, especially in cases with indistinct borders or structurally similar lesions. Additionally, previous models lacked both a global receptive field and high computational efficiency. In this work, we present the XLSTM-VMUNet Model, which jointly capture spatial and sequential features within derma-tological images successfully. XLSTM-VMUNet can not only specialize in extracting spatial features from images, focusing on the structural characteristics of skin lesions, but also enhance contextual understanding, allowing more effective handling of complex medical image structures. Experiment results on the ISIC2018 dataset demonstrate that XLSTM-VMUNet outperforms VMUNet by 1.25% on DSC and 2.07% on IoU, with faster convergence and consistently high segmentation perfor-mance. Our code of XLSTM-VMUNet is available at https://github.com/FangZhuoyi/XLSTM-VMUNet.

1. Introduction

As the largest organ in the human body, the skin acts as the primary barrier against ultraviolet radiation, safe-guarding the body from its detrimental effects [1]. The 2023 global cancer statistics indicate that malignant skin lesions account for tens of thousands of deaths each year [2]. Notably, melanoma, a highly aggressive type of skin cancer, is rapidly becoming one of the fastest-increasing cancers around the world [3,4,5,6,7]. Segmentation plays a vital and challenging role in the workflow for automated skin lesion analysis [8]. In recent years, a large number of computer-assisted segmentation techniques have been developed for medical images. However, segmenting medical image automatically and accurately is a literally challenging task because these images are inherently complex and rarely contain simple linear features [9]. Over the past decade, numerous studies have focused on the develop-ment of efficient and robust segmentation methods for medical imaging. Among these contributions, U-Net [10,11,12] stands out as a seminal work that first illustrated the efficacy of encoder-decoder convolutional networks with skip connections for medical image segmentation, and it has also yielded promising outcomes in various image translation tasks. Since the inception of U-Net [16], a number of significant modifications have emerged [13,14,15], particularly within the domain of medical imaging, including variants such as U-Net++ [17], 3D U-Net [18], V-Net [19], and Ynet [20]. Additionally, UneXt [21], Rolling-UNet [22], HEA-Net [23] and U-MLP [24] incorporate hybrid methodologies that combine convolu-tional operations with multi-layer perceptrons (MLP) to enhance the performance of segmentation networks, thereby facilitating their application in resource-limited point-of-care settings. Recently, a variety of networks leveraging Convolutional Neural Networks (CNN) [25,26,27,28,29] and Vision Transformers (ViT) [30] have been employed to augment the U-Net archi-tecture for medical image segmentation. These networks have proven effective in addressing global context and long-range dependencies within the segmentation tasks. In comparison to CNN, ViT typically exhibits enhanced learning capabi-lities on large-scale medical image seg-mentation datasets [31], attributed to its incorporation of the self-attention mechanism [32,33,34]. However, the quadratic complexity associated with the self-attention mechanism, coupled with the substantial number of tokens, results in significant computational overhead when applied to large-scale skin lesion image segmentation tasks that involve high spatial resolutions [35,36,37,38]. The unre-solved trade-off bet-ween achieving a global receptive field and maintaining high computational efficiency drives the need for a novel architecture tailored for large-scale skin lesion image segmentation, which aims to retain the intrinsic benefits of the standard self-attention mechanism, including global receptive fields and dynamic weighting parameters.

State Space Models (SSM) [39,40,41,42] have attracted significant interest owing to their computational efficiency Mamba [43], a novel SSM within the realm of natural

language processing (NLP) [44,45], has emerged as a highly promising method for modeling long sequences with linear complexity [46]. Due to its advantages over conventional foundational architectures, Mamba holds significant potential as a visual foundational architecture [47,48]. It has been actively utilized across various computer vision tasks [49], contributing notably to the field of medical image segmentation [50]. Inspired by Mamba, Vision Mamba [51] and Visual Mamba [52] were the pioneering implementations of this model in the visual domain, achieving very impressive results. Furthermore, several researchers have adapted it for medical image segmentation, resulting in innovations such as VM-Unet [53], U-Mamba [54], H-vmunet [55], Swin-Umamba [56], nnMamba [57], Mamba-UNet [58], LightM-Unet [59] and UltraLight-VM-UNet [60]. Particularly, SkinMamba [61] facilitates expert knowledge exchange across different levels in a global state and achieves high-frequency restoration and boundary prior guidance.

However, the challenges remaining in skin lesion segmentation have not been solved completely. For instance, existing models exhibit limitations in simultaneously capturing spatial and sequential features, which hampers their ability to comprehensively understand the information within skin lesion images. Additionally, these models lack contextual understanding, making it challenging to establish long-range dependencies when processing skin lesion images. Previous methods also struggle to achieve precise segmentation in the presence of ambiguous boundaries or similar structures, resulting in inadequate extraction of detailed spatial features, particularly in addressing subtle structures and lesion boundaries. Furthermore, these methods find it difficult to balance global receptive fields with high computational efficiency.

Recently, the Extended Long Short-Term Memory (xLSTM) [62] architecture represents a significant advancement in language modeling, demonstrating potential to compete with Transformer and State SSM. By optimizing the performance of Long Short-Term Memory (LSTM) [63,64,65,66,67], xLSTM effectively manages long-range dependencies while maintaining linear com-putational and memory efficiency [68,69]. Similar to models such as ViT in the field of computer vision, xLSTM offers a powerful alternative in the evolving landscape of medical image segmentation [70,71,72]. Vision-LSTM [73] employed a generic computer vision backbone that uses xLSTM blocks as its core components. xLSTM-UNet [74] proposed the xLSTM-enabled U-Net image segmentation network that can perform both 2D and 3D medical image segmentation tasks and achieves state-of-theart (SOTA) results.

In this paper, we propose the XLSTM-VMUNet model, which combines Mamba with xLSTM for efficient skin lesion segmentation. Through a carefully designed architecture, our model excels in feature extraction, memory

retention, adaptability, and nonlinear modeling. First, we leverage Mamba for deep spatial feature extraction using a multi-layer convolutional and pooling network to progressively capture essential features from skin lesion images. The integration of residual connections enhances feature transfer efficiency and improves processing capability for complex lesion patterns, establishing a robust basis for xLSTM. Following feature extraction, we input spatial features into xLSTM to utilize its long-term and short-term memory mechanisms. xLSTM processes sequential data while preserving crucial contextual information via a detailed state update mechanism. Specifically, we designed gating mechanisms that allow the model to selectively retain key features during skin lesion processing, maintaining segmentation performance across varying lesion types. To boost adaptability, we incorporated structured input processing in xLSTM, including a BlockDiagonal structure, to address diverse skin lesion types. This dynamic feature adjustment enables the model to adapt flexibly to the varying characteristics and distributions of different lesion categories, a crucial capability given the diverse morphology and sizes found in skin lesions. Finally, for feature fusion, we implemented a multi-level feature integration mechanism, combining Mamba-extracted features with xLSTM's output through concatenation and weighted fusion. This strategy enhances segmentation accuracy and improves pattern recognition. We employed cross-validation during validation to ensure stability and reliability across different skin lesion datasets.

In summary, the following are the major contributions of our work:

◆ We introduce the XLSTM-VMUNet model, which is designed to efficiently extract and integrate both spatial features and temporal information within skin lesion images. By leveraging the strengths of xLSTM in modeling long-range dependencies and temporal dynamics, our XLSTM-VMUNet model significantly improves the accuracy and robustness of the segmentation process.

◆ We propose a multi-level feature integration mechanism to effectively combine the features extracted by Mamba with the processing results of xLSTM. The feature linking and weighted fusion ensures that feature information at different levels can be fully integrated, which significantly improves the accuracy of the model for skin lesion seg-mentation and enhances the ability of the model to capture complex patterns.

◆ We conduct extensive experiments conducted on the ISIC2018 skin lesion segmentation dataset, demonstrating that XLSTM-VMUNet outperforms SOTA (state-of-the-art) methods across Dice and IoU metrics, with faster convergence and consistently high segmentation perfor-mance.

2. Related Work

2.1. Medical image segmentation

Medical images play a pivotal role in aiding healthcare providers in diagnosis and treatment decisions [75,76]. Interpretation relies on radiologists' expertise, which is time-intensive and subjective, influenced by experience and training [77]. Therefore, integrating computer-aided systems has become crucial to ensure efficient, objective, and consistent analysis of medical images [94,95,96]. Image segmentation, a key process in medical physics, is essential for identifying tumors or lesions by partitioning an image into homogeneous regions for extracting diagnostic information [97,98,99]. Advanced techniques have been developed to address the limitations of traditional methods, significantly improving both accuracy and efficiency in medical image analysis [80,81,82,100].

Since the introduction of U-Net, several variants have been proposed to enhance its performance. U-Net++ [17] replaces traditional cropping and concatenation with dense convolutions, improving feature fusion and reducing information loss. Attention-U-Net [102] integrates attention mechanisms to focus on relevant regions and suppress irrelevant information. Res-U-Net [101] introduces residual blocks to stabilize feature transfer and improve deep network training. Dense-U-Net [103,104] employs Denseblocks for efficient feature reuse and better multi-scale information capture. U-Netv2 [105] uses an innovative skip connection mechanism to refine feature fusion and improve integration across scales.

2.2. Mamba

Mamba, based on the SSM [39], provides a more efficient alternative to transformers in medical image analysis [40]. With linear time complexity, it processes longer sequences faster, reduces memory usage, and excels in multimodal data integration, enhancing diagnostic accuracy and patient outcomes [41,42].

Vim (Zhu et al., 2024a) [51] is a Mamba-based architecture that processes image patch sequences, using position embeddings and a class token. The sequence is then passed through Vim blocks with both forward and backward SSM paths. VMamba (Liu et al., 2024g) [52] enhances Mamba's 1D scanning by introducing the Cross-Scan Module (CSM), which scans image patches in four directions and applies selective SSMs to capture cross-directional dependencies. The sequences are merged back into the original 2D layout. It uses stacked VSS blocks with down-sampling, where the vanilla VSS block replaces 1D convolution with 2D depthwise convolution and incorporates SS2D with layer normalization. PlainMamba (Yang et al., 2024a) [83] is a non-hierarchical architecture optimized for multi-scale fusion, multi-modal integration, and hardware efficiency. It processes 2D patches with depthwise convolutions and adapted selective scanning using zigzag and direction-aware updates.

LocalMamba (Huang et al., 2024e) [106] resolves local token dependency issues by dividing the image into local windows for directional selective scanning (SSM), while maintaining global SSM. It also uses spatial and channel attention before patch merging and optimizes scan directions for each layer to improve efficiency. Efficient-VMamba (Pei et al., 2024) [107] combines Efficient 2D Scanning (ES2D) with atrous sampling and a convolutional branch for global and local feature extraction, processed by a Squeeze-and-Excitation (SE) block [108]. The output forms the EVSS block, with EVSS in early stages and Inverted Residual blocks in later stages.

2.3. xLSTM

The xLSTM [62] model marks a significant breakthrough in the field of sequence modeling, offering a powerful alternative to established architectures like Transformer and SSM, which have dominated machine learning applications in natural language processing and computer vision. Building upon traditional Long Short-Term Memory (LSTM) networks [63,64,65,66,67], xLSTM introduces key innovations that enable efficient capture of long-range dependencies, all while maintaining linear computational complexity and memory efficiency. This makes xLSTM particularly well-suited for scenarios involving large-scale datasets and high-dimensional inputs, where conventional RNN models often encounter scalability and performance limitations.

xLSTM presents a promising alternative to traditional convolutional methods in medical image segmentation, a field that demands high precision and effective multi-scale feature integration. The Vision-LSTM model [73] exemplifies this approach by embedding xLSTM blocks into a general-purpose computer vision architecture, improving the model's ability to capture both spatial and temporal dependencies within medical images. This integration enhances feature representation, enabling more accurate differentiation of subtle patterns, such as tumor structures and organ boundaries.

Furthermore, the xLSTM-UNet architecture [74], which integrates xLSTM units with the U-Net framework, has demonstrated outstanding performance in both 2D and 3D medical image segmentation tasks. By harnessing xLSTM's ability to model long-range dependencies, xLSTM-UNet enhances the network's capacity to capture global contextual information, thereby improving segmentation accuracy, particularly in complex cases with intricate anatomical structures or heterogeneous tissue types.
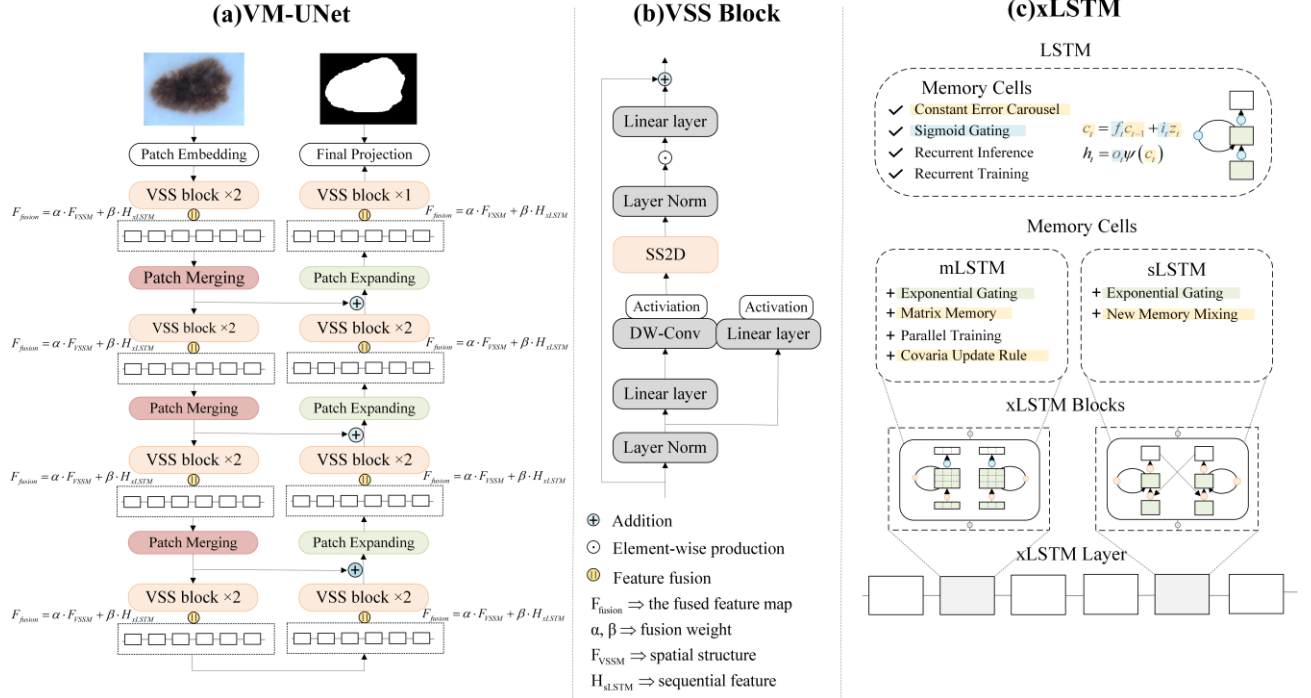
Figure 1. The Architecture Overview of XLSTM-VMUNet.

3. Method

Firstly, we introduce selective state space models (S6). Then, we describe the VSS block and the xLSTM block. Finally, we ascensively elaborate on the core structure: the XLSTM-VMUNet Model.

3.1. SSM

SSM is a core class of framework in deep learning for processing sequential data. These models aim to map an input sequence, denoted as $x(t)$, from a real vector space R^L to an output sequence $y(t)$ within the same space, while leveraging an intermediate latent state $h(t)$ also within R^N. The system dynamics are governed b a series of linear transformations, as outlined in the corresponding set of equations:

$$\begin{cases} h'(t) = Ah(t) + Bx(t) \\ y(t) = Ch(t) \end{cases}, \quad (1)$$

where A, B, and C are system matrices of suitable dimensions that govern the state transition dynamics, the influence of the input, and the mapping to the output, respectively. These matrices are defined as $A \in \mathbb{R}^{N \times N}$, $B \in \mathbb{R}^{N \times 1}$, and $C \in \mathbb{R}^{N \times 1}$.

For practical implementation, the continuous-time model is discretized using a zero-order hold approximation, converting the system matrices A and B into their discrete counterparts over a sampling period Δ. The discretized system is represented as:

$$\begin{cases} \overline{A} = e^{\Delta A} \\ \overline{B} = (\Delta A)^{-1}(e^{\Delta A} - I) \cdot \Delta B \end{cases}. \quad (2)$$

The resulting equations for the discrete model are given by:

$$\begin{cases} h_t = \overline{A}h_{t-1} + \overline{B}x_t \\ y_t = Ch_t \end{cases}. \quad (3)$$

To improve efficiency, the entire sequence output can be computed simultaneously using a global convolution, boosting both scalability and speed. This is formulated as:

$$\begin{cases} y = x \otimes \overline{K} \\ \overline{K} = \left(C\overline{B}, C\overline{AB}, \ldots, C\overline{A}^{L-1}\overline{B} \right) \end{cases}, \quad (4)$$

where $\otimes$ denotes the convolution operation, L represents the sequence length, and $\overline{K}$ is the kernel derived from the SSM, specifically tailored for efficient sequence processing.

3.2. Selective State Space Models (S6)

The linear time-invariant state-space model treats all tokens equally, neglecting dynamic content importance. Prioritizing more relevant tokens and adjusting attention accordingly is more effective for complex inputs.

Mamba integrates a selectivity mechanism into the state-space model, creating Selective State Space Models (S6). It applies the SSM independently across each channel of an input sequence with batch size B, length L, and D channels.

In Mamba, the matrices B, C, and Δ are input-dependent, allowing adaptive behavior. The discretization process with the selectivity mechanism is as follows:

$$\begin{cases} \overline{B} = s_B(x) \\ \overline{C} = s_C(x) \\ \Delta = \tau_A(\Delta + s_A(x)) \end{cases}, \qquad (5)$$

where $\overline{B} \in \mathbb{R}^{B \times L \times N}$, $\overline{C} \in \mathbb{R}^{B \times L \times N}$ and $\Delta \in \mathbb{R}^{B \times L \times D}$. $s_B(x)$ and $s_C(x)$ are linear functions that project the input x into a N-dimensional space, while $s_A(x)$ projects the hidden state dimension D linearly into the desired dimension, connected to the RNN gating mechanism. These computations transform Δ, B, and C into input-dependent functions of length L, converting the time-invariant model into a time-varying one and enabling selectivity.

The parameter Δ is expanded to (B, L, D), giving each token in a batch a unique input-dependent control. A larger step size for Δ prioritizes the input, while a smaller one emphasizes the stored state. Parameters B and C become input-dependent, refining the control between input x, state h, and output y. While A remains independent, its relevance to the input is introduced via Δ's data dependency. With dimension N, A adapts across SSM dimensions, enabling precise generalization.

3.3. VSS Block

The VSS Block, derived from VMamba, is central to XLSTM-VMUNet. After Layer Normalization, the input splits into two branches: one applies a linear layer, the other adds depthwise separable convolution and uses the 2D-Selective-Scan (SS2D) module. The branches are fused, normalized, and merged with a residual connection, using SiLU as the activation.

SS2D unfolds the input in four directions, processes it in the S6 block, and merges it back, enhancing selectivity by adjusting parameters to capture key features and reduce noise. Figure 2 reveals the scan expanding operation and the scan merging operation in SS2D.
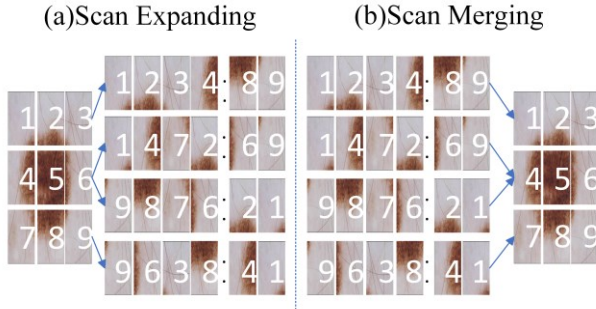

Figure 2. (a) The scan expanding operation in SS2D. (b) The scan merging operation in SS2D.

3.4. xLSTM Block

3.4.1. sLSTM Block

The sLSTM Block extends the traditional LSTM architecture by introducing exponential gating and normalization states to enhance the control over information storage and flow.

● **Memory Cell and State Update**

The memory cell is updated as follows:

$$\begin{cases} c_t = f_t c_{t-1} + i_t z_t \\ z_t = tanh(W_z x_t + R_z h_{t-1}) \end{cases}, \qquad (6)$$

where c_t is the memory cell at time step t, f_t and i_t are the forget and input gates respectively, z_t is the candidate memory, controlled by W_z and R_z.

Normalization state update:

$$n_t = f_t n_{t-1} + i_t, \qquad (7)$$

where n_t is the normalization state that balances the contribution of the forget and input gates.

The hidden state is computed as:

$$\begin{cases} h_t = \dfrac{o_t c_t}{n_t} \\ o_t = \sigma(W_o x_t + R_o h_{t-1}) \end{cases}, \qquad (8)$$

where o_t is the output gate, controlling the final output h_t. Normalizing c_t by n_t ensures numerical stability.

● **Projection and Residual Connection**

The hidden state is further processed through up-projection, non-linear transformation, and down-projection:

$$\begin{cases} y_{left} = W_{up-left} h_t \\ y_{right} = W_{up-right} h_t \\ y_{gated} = GELU(y_{right}) \\ y_{out} = W_{down}(y_{left} \cdot y_{gated}) \end{cases}. \qquad (9)$$

The final output includes a residual connection:

$$F = y_{out} + x, \qquad (10)$$

where F represents the final output.

3.4.2. mLSTM Block

The mLSTM Block augments memory capacity by extending the memory cell from a scalar to a matrix, thereby enabling more complex storage and representation.

● Matrix Memory and Key-Value Storage

The memory cell is updated in matrix form:

$$\begin{cases} C_t = f_t C_{t-1} + i_t v_t k_t^T \\ k_t = \dfrac{1}{\sqrt{d}} W_k x_t + b_k \\ v_t = W_v x_t + b_v \end{cases}, \qquad (11)$$

where C_t is the memory matrix, v_t and k_t are the value and key vectors respectively, W_k, W_v are the weights for generating key and value vectors, b_k, b_v are the biases.

● Memory Retrieval and Normalization

To retrieve information from the matrix memory, mLSTMBlock uses a query vector q_t:

$$\begin{cases} h_t = o_t \odot \dfrac{C_t q_t}{max(|n_t^T q_t, 1|)} \\ q_t = W_q x_t + b_q \\ n_t = f_t n_{t-1} + i_t k_t \end{cases}, \qquad (12)$$

where q_t is the query vector and n_t is the normalization state.

The matrix-based memory update and the retrieval mechanism significantly enhance the model's ability to capture complex temporal relationships. By effectively managing and retaining information across time steps, it preserves long-term dependencies. This dynamic memory adjustment improves the model's capacity to model intricate temporal patterns, which is crucial for tasks involving sequential data, where understanding complex dependencies is essential for accurate modeling.

3.5. XLSTM-VMUNet

3.5.1. VSSM Feature Extraction

The architecture integrates the VSSM with the xLSTM component through the XLSTM-VMUNet framework.

The Visual Structured State Model (VSSM) is responsible for extracting deep spatial features from the input image. Given an input image $x \in \mathbb{R}^{H \times W \times C}$, VSSM utilizes multiple convolution and pooling layers to progressively extract essential features.

For a given layer l, let $F^{(l)}$ denote the feature map after convolution. The convolution operation in VSSM is defined as:

$$F^{(l)} = \sigma\big(W^{(l)} \otimes F^{(l-1)} + b^{(l)}\big), \qquad (13)$$

where $W^{(l)}$ represents the weight matrix of layer l, $b^{(l)}$ is the bias term for layer l, $\otimes$ denotes the convolution operation, σ is the activation function (e.g., ReLU), and x is the input image.

Through these layered convolutions, VSSM produces a set of multi-scale spatial features, denoted as $\big\{F_{VSSM}^{(1)}, F_{VSSM}^{(2)}, \ldots, F_{VSSM}^{(L)}\big\}$, where each $F_{VSSM}^{(l)}$ spatial information at different scales, providing rich representations for subsequent sequence modeling.

3.5.2. Sequence Modeling with xLSTM

Following spatial feature extraction, the xLSTM network is employed to model long short-term dependencies.

Let the spatial features from VSSM be $F_{VSSM} = \big\{F_{VSSM}^{(1)}, \ldots, F_{VSSM}^{(L)}\big\}$, where each $F_{VSSM}^{(l)}$ represents a timestep in the sequence.

The xLSTM state update equations are:

$$\begin{cases} i_t = \sigma\big(W_i \cdot F_{VSSM}^{(t)} + U_i \cdot h_{t-1} + b_i\big) \\ f_t = \sigma\big(W_f \cdot F_{VSSM}^{(t)} + U_i \cdot h_{t-1} + b_f\big) \\ o_t = \sigma\big(W_o \cdot F_{VSSM}^{(t)} + U_o \cdot h_{t-1} + b_o\big) \\ g_t = tanh\big(W_g \cdot F_{VSSM}^{(t)} + U_g \cdot h_{t-1} + b_g\big) \end{cases}, \qquad (14)$$

where i_t, f_t and o_t denote the input gate, forget gate, and output gate at timestep t respectively, g_t represents the candidate state, W_i, W_f, W_o, W_g are weight matrices for the gates, U_i, U_f, U_o, U_g are weight matrices associated with the hidden state h_{t-1} from the previous timestep, b_i, b_f, b_o, b_g are bias vectors, σ is the sigmoid activation function.

The cell state c_t and hidden state h_t are updated as follows:

$$\begin{cases} c_t = f_t \odot c_{t-1} + i_t \odot g_t \\ h_t = o_t \odot tanh(c_t) \end{cases}, \qquad (15)$$

where c_t is the cell state at timestep t, h_t represents the hidden state at timestep t, $\odot$ denotes the element-wise multiplication, $tanh$ is the hyperbolic tangent activation function.

This gating mechanism enables xLSTM to selectively retain or forget spatial features, which is critical for preserving long-term dependencies and contextual information across sequential image data.

3.5.3. Multi-level Feature Fusion

The model employs a multi-level feature fusion mechanism to combine the spatial features from VSSM and temporal features from xLSTM, resulting in a comprehensive representation. Let F_{VSSM} be the spatial feature map from VSSM, and H_{xLSTM} be the hidden state output from xLSTM. The fused feature map F_{fusion} is given by:

$$F_{fusion} = \alpha \cdot F_{VSSM} + \beta \cdot H_{xLSTM}, \qquad (16)$$

where F_{fusion} represents the fused feature map that combines spatial and temporal information, α and β are fusion weights, determining the contributions of F_{VSSM} and H_{xLSTM} to the fused feature, F_{VSSM} captures spatial structure, and H_{xLSTM} captures sequential and memory-dependent features.

This fusion strategy enables the model to capture complex patterns across both spatial and temporal domains, enhancing segmentation performance on challenging data.

3.5.4. Loss function

The introduction of XLSTM-VMUNet is designed to evaluate the potential benefits of combining Mamba with

xLSTM for more efficient skin lesion segmentation. In this context, we focus solely on the most fundamental loss functions, namely Binary Cross-Entropy and Dice loss (denoted as BceDice loss), for the skin lesion segmentation task. These loss functions are formally represented in Equations 17.

$$L_{BceDice} = \lambda_1 L_{Bce} + \lambda_2 L_{Dice}, \qquad (17)$$

$$\begin{cases} L_{Bce} = -\dfrac{1}{N}\sum_{i=1}^{N}[y_i log(\hat{y}_i) + (1-y_i)log(1-\hat{y}_i)] \\ L_{Dice} = 1 - \dfrac{2|X \cap Y|}{|X| + |Y|} \end{cases} , (18)$$

where N denotes the total number of samples, y_i, $\hat{y}_i$ respectively signify the true label and prediction. $|X|$ and $|Y|$ represent the ground truth and prediction, respectively. λ_1, λ_2 refer to the weights of loss functions, which are both set to 1 by default.

4. Experiments

4.1. Dataset

The dermoscopic images utilized for both training and evaluation were derived from the ISIC 2018 Machine Learning Challenge (ISIC 2018: Skin Lesion Analysis for Melanoma Detection) [109,110,111]. The training dataset consists of 8,010 samples, which are categorized into seven distinct disease classes. For the evaluation phase, a subset of 161 samples was selected from the original training set [112,113,114]. The lesion images were sourced from the HAM10000 dataset, which is publicly accessible via both the archive gallery and standardized API endpoints. Throughout the ISIC 2018 challenge, image data, along with corresponding diagnostic information and ground-truth labels, were made available for download. The competition is organized around three separate tasks, each addressing different facets of skin lesion analysis, providing a comprehensive evaluation of model performance in melanoma detection:
- Task 1: Lesion Segmentation,
- Task 2: Lesion Attribute Detection,
- Task 3: Disease Classification.

In this study, we focus on Task 1 of the ISIC 2018: Skin Lesion Analysis for Melanoma Detection grand challenge.

4.2. Implementation Details

The images from the ISIC2018 dataset are preprocessed to a resolution of 256×256 pixels before being fed into the model. Training is conducted with a batch size of 8, utilizing the AdamW optimizer [92] with an initial learning rate of 1×10^{-3}. In order to facilitate dynamic learning rate adjustments throughout the training process, a Cosine-AnnealingLR scheduler [93] is employed. All experiments

are conducted on a single NVIDIA TESLA A100-PCIE-40GB GPU for 150 epochs, providing the computational power necessary for efficient training and evaluation.
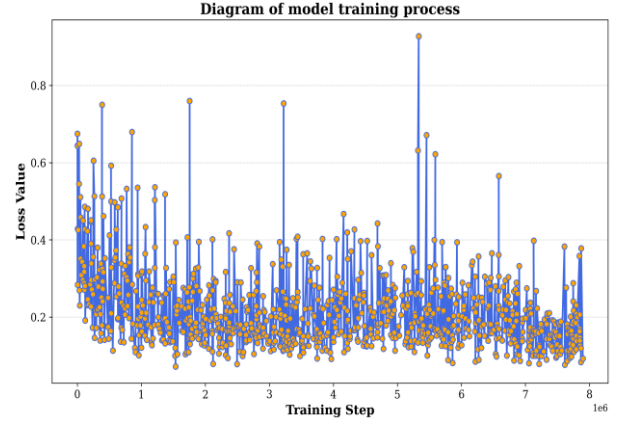

Figure 3. The diagram of the training process of our XLSTM-VMUNet Model.

Table 1. Comparison with state-of-the-art methods, 5-fold cross-validation. (Bold indicates the best.)

Model	DSC↑	IoU↑
R2U-Net [84]	0.6790	0.5810
Attention R2U-Net [89]	0.7260	0.5920
Attention-U-Net [102]	0.8205	0.7346
U-Net [16]	0.8403	0.7455
U-Net++ [17]	0.8496	0.7512
Swin-U-Net [85]	0.8523	0.7528
Res-U-Net [100]	0.8560	0.7562
CaraNet [86]	0.8702	0.7822
FANet [90]	0.8731	0.8023
PraNet [87]	0.8754	0.7874
VM-UNetv2 [88]	0.8796	0.7851
UltraLight VM-UNet [60]	0.8820	0.7890
TransUNet [91]	0.8891	0.8051
VM-UNet [53]	0.8975	0.8142
SkinMamba [61]	0.8976	0.8143
UNeXt [21]	0.9030	0.8261
XLSTM-VMUNet	**0.9100**	**0.8349**

4.3. Results

Segmentation performamnce. In order to demonstrate the effective of our proposed approach, we conducted a comparative analysis of XLSTM-VMUNet against other state-of-the-art methodologies. Specifically, they include R2U-Net [84], Attention R2U-Net [89], Attention-U-Net [102], U-Net [16], U-Net++[17], Swin-U-Net [85], Res-U-Net [101][, CaraNet [86], FANet [90], PraNet [87], VM-UNetv2 [88], UltraLight VM-Unet [60], TransUNet [91], VM-UNet [53], SkinMamba [61] and UNeXt [21].

Table 1 provides a comparative analysis of the results on the ISIC2018 dataset, demonstrating that the proposed XLSTM-VMUNet outperforms other models, particularly in terms of the Dice Similarity Coefficient (DSC) and Intersection over Union (IoU). The model training process is illustrated in Figure 3, while Figure 4 presents a visual comparison of the segmentation results.
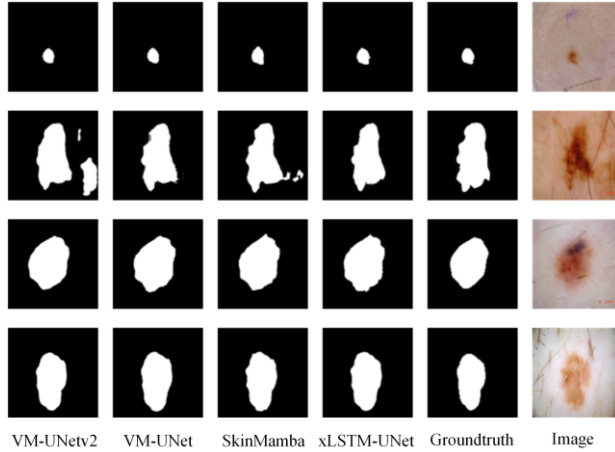

Figure 4. Visualized segmentation results of the proposed XLSTM-VMUNet against other state-of-the-arts over the ISIC2018 dataset

From the Figure 4, it is evident that the proposed XLSTM-VMUNet model exhibits a markedly improved sensitivity to fine lesion details compared to conventional methods. By effectively capturing multi-scale contextual information and leveraging temporal dependencies, XLSTM-VMUNet is able to detect subtle variations in lesion characteristics, thereby improving the accuracy and precision of lesion delineation. This capability is particularly critical in medical image analysis, where accurate segmentation of lesions is essential for reliable diagnosis and treatment planning.

Ablation study. We conducted an ablation study on the ISIC2018 dataset to examine the effectiveness of our modules under various configurations as summarized in Table 2. The trend plot of the four versions of our XLSTM-VMUNet Model is shown in Figure 5. Comparison of Dice and IoU values across XLSTM-VMUNet versions is shown in Figure 6.

Table 2. Ablation experiments: impact of individual contributions on segmentation performance of XLSTM-VMUNet. (Bold indicates the best.)

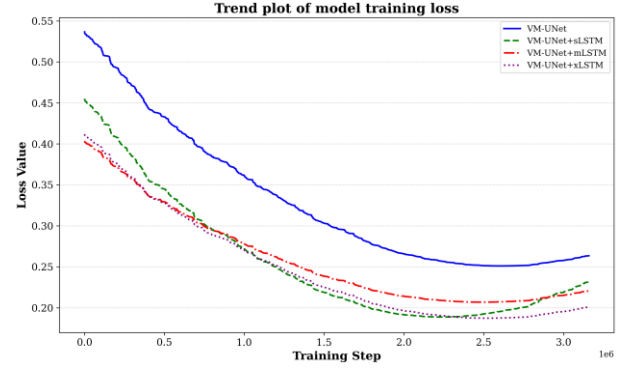| Ver.	sLSTM	mLSTM	DSC↑	IoU↑
Ver 1	✗	✗	0.8975	0.8142
Ver 2	✓	✗	0.9013	0.8238
Ver 3	✗	✓	0.9098	0.8345
Ver 4	✓	✓	0.9100	0.8349

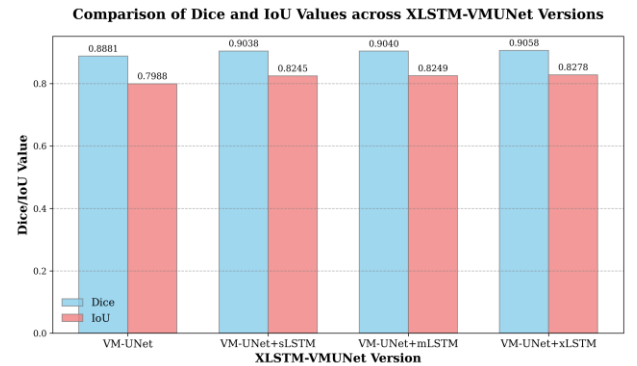Figure 5. The trend plot of the four versions of our XLSTM-VMUNet Model.

Figure 6. Comparison of Dice and IoU values across XLSTM-VMUNet versions.

From Figure 5 and Figure 6, we can indicate that combining VM-UNet with xLSTM shows outstanding performance in converging quickly and maintaining optimal segmentation performance among the four versions of our XLSTM-VMUNet Model.

5. Conclusion

In this study, we propose the XLSTM-VMUNet model and demonstrate the benefits of effectively combining Mamba with xLSTM: XLSTM-VMUNet can not only focus on extracting spatial features from images, especially the structure and characteristics of skin lesions, but also enhance the model's contextual understanding, allowing it to better handle complex structures in medical images. This dual integration significantly improves the accuracy of skin lesion segmentation and enhances the model's computational efficiency. Experimental results indicate that on the ISIC2018 dataset, XLSTM-VMUNet outperforms UNeXt with a 0.70% improvement in the DSC metric and a 0.88% improvement in the IoU metric. Compared to the baseline model, VM-UNet, XLSTM-VMUNet shows a 1.25% increase in the DSC metric and a 2.07% increase in the IoU metric.

References

[1] Ibrahim Abdulrab Ahmed, Bakri Awaji, Fekry Olayah, and Ebrahim Mohammed Senan. AI techniques of dermoscopy image analysis for the early detection of skin lesions based on combined CNN features[J]. Diagnostics, 2023, 13(7): 1314.

[2] Erin Clancy. ACS Report Shows Prostate Cancer on the Rise, Cervical Cancer on the Decline[J]. Renal & Urology News, 2023: NA-NA.

[3] Xianghua Xie, and Feng Zhao. An overview of interactive medical image segmentation[J]. Annals of the BMVA, 2013, 2013(7): 1-22.

[4] Heang-Ping Chan, Lubomir M. Hadjiiski, and Ravi K. Samala. Computer-aided diagnosis in the era of deep learning[J]. Medical physics, 2020, 47(5): e218-e227.

[5] Samuel G Armato 3rd, Kenny Cha, Kenny Cha, Quan Chen, Karen Drukker, Lubomir Hadjiiski, Henkjan Huisman, Zhimin Huo, Richard Mazurchuk, Janne J Näppi, et al. AAPM task group report 273: recommendations on best practices for AI and machine learning for computer-aided diagnosis in medical imaging[J]. Medical Physics, 2023, 50(2): e1-e24.

[6] Esther E Bron, Rose Bruffaerts, Randy L Gollub, Juan Eugenio Iglesias, Hyungsoon Im, Matthew J Leming, and Yangming Ou.Challenges of implementing computer-aided diagnostic models for neuroimages in a clinical setting[J]. NPJ Digital Medicine, 2023, 6(1): 129.

[7] Junkai Ji, Cheng Tang, and Yajiao Tang. A novel machine learning technique for computer-aided diagnosis[J]. Engineering Applications of Artificial Intelligence, 2020, 92: 103627.

[8] Kumar Abhishek, Sandra Avila, Catarina Barata, Alceu Bissoto, M Emre Celebi, Ghassan Hamarneh, Zahra Mirikharaji, and Eduardo ValleA. survey on deep learning for skin lesion segmentation[J]. Medical Image Analysis, 2023, 88: 102863.

[9] Lalit M Aggarwal, and Neeraj Sharma. Automated medical image segmentation techniques[J]. Journal of medical physics, 2010, 35(1): 3-14.

[10] M. Krithika alias AnbuDevi, and K. Suganthi. Review of semantic segmentation of medical images using modified architectures of UNET[J]. Diagnostics, 2022, 12(12): 3064.

[11] Xu Cao, Xueli Chen, Getao Du, Jimin Liang, and Y. Zhan. Medical Image Segmentation based on U-Net: A Review[J]. Journal of Imaging Science & Technology, 2020, 64(2).

[12] Jianhong Cheng, Liangliang Liu, Quan Quan, Jianxin Wang, Yuping Wang, and Fangxiang Wu. A survey on U-shaped networks in medical image segmentations[J]. Neurocomputing, 2020, 409: 244-258.

[13] Vijay Devabhaktuni, Colin P. Elkin, Nahian Siddique, and Sidike Paheding. U-net and its variants for medical image segmentation: A review of theory and applications[J]. IEEE access, 2021, 9: 82031-82057.

[14] Ehsan Khodapanah Aghdam, Atlas Haddadi Avval, Reza Azad, Afshin Bozorgpour, Yiwei Jia, and Amelie Rauland. Medical image segmentation review: The success of u-net[J]. IEEE Transactions on Pattern Analysis and Machine Intelligence, 2024.

[15] M. Krithika alias AnbuDevi, and K. Suganthi. "Review of semantic segmentation of medical images using modified architectures of UNET." Diagnostics 12.12 (2022): 3064.

[16] Thomas Brox, Philipp Fischer, and Olaf Ronneberger. U-net: Convolutional networks for biomedical image segmentation[C]//Medical image computing and computer-assisted intervention–MICCAI 2015: 18th international conference, Munich, Germany, October 5-9, 2015, proceedings, part III 18. Springer International Publishing, 2015: 234-241.

[17] Jianming Liang, Md Mahfuzur Rahman Siddiquee, Nima Tajbakhsh, and Zongwei Zhou. Unet++: A nested u-net architecture for medical image segmentation[C]//Deep Learning in Medical Image Analysis and Multimodal Learning for Clinical Decision Support: 4th International Workshop, DLMIA 2018, and 8th International Workshop, ML-CDS 2018, Held in Conjunction with MICCAI 2018, Granada, Spain, September 20, 2018, Proceedings 4. Springer International Publishing, 2018: 3-11.

[18] Ahmed Abdulkadir, Thomas Brox, Özgün Çiçek, Soeren S. Lienkamp, and Olaf Ronneberger. 3D U-Net: learning dense volumetric segmentation from sparse annotation[C]//Medical Image Computing and Computer-Assisted Intervention–MICCAI 2016: 19th International Conference, Athens, Greece, October 17-21, 2016, Proceedings, Part II 19. Springer International Publishing, 2016: 424-432.

[19] Seyed-Ahmad Ahmadi, Fausto Milletari, and Nassir Navab. V-net: Fully convolutional neural networks for volumetric medical image segmentation[C]//2016 fourth international conference on 3D vision (3DV). Ieee, 2016: 565-571.

[20] Azade Farshad, Peter Gehlbach, Nassir Navab, and Yousef Yegane. Y-net: A spatiospectral dual-encoder network for medical image segmentation[C]//International Conference on Medical Image Computing and Computer-Assisted Intervention. Cham: Springer Nature Switzerland, 2022: 582-592.

[21] Vishal M. Patel, and Jeya Maria Jose Valanarasu. Unext: Mlp-based rapid medical image segmentation network[C]//International conference on medical image computing and computer-assisted intervention. Cham: Springer Nature Switzerland, 2022: 23-33.

[22] Zihan Chen, Jie Gao, Mengting Liu, Yutong Liu, Huaiyuan Yu, and Haijiang Zhu. Rolling-Unet: Revitalizing MLP's Ability to Efficiently Extract Long-Distance Dependencies for Medical Image Segmentation[C]//Proceedings of the AAAI Conference on Artificial Intelligence. 2024, 38(4): 3819-3827.

[23] Lijing An, Yongming Li, and Liejun Wang. HEA-Net: attention and MLP hybrid encoder architecture for medical image segmentation[J]. Sensors, 2022, 22(18): 7024.

[24] Shuo Gao, Airong Qian, Menglei Xu, Wenhui Yang, Hong Yu, Hao Zhang, and Wenjuan Zhang. U-MLP: MLP-based ultralight refinement network for medical image segmentation[J]. Computers in Biology and Medicine, 2023, 165: 107460.

[25] Jianfei Cai, Tsuhan Chen, Jiuxiang Gu, Jason Kuen, Ting Liu, Lianyang Ma, Amir Shahroudy, Bing Shuai, Gang Wang, Xingxing Wang, et al. Recent advances in convolutional neural networks[J]. Pattern recognition, 2018, 77: 354-377.

[26] Fan Liu, Zewen Li, Shouheng Peng, Wenjie Yang, and Jun Zhou. A survey of convolutional neural networks: analysis, applications, and prospects[J]. IEEE transactions on neural networks and learning systems, 2021, 33(12): 6999-7019.

[27] Ryan Nash, and Keiron O'Shea. An introduction to convolutional neural networks[J]. arXiv preprint arXiv:15-11.08458, 2015.

[28] Richard Kinh Gian Do, Mizuho Nishio, Kaori Togashi , and Rikiya Yamashita. Convolutional neural networks: an overview and application in radiology[J]. Insights into imaging, 2018, 9: 611-629.

[29] Jianxin Wu. Introduction to convolutional neural networks[J]. National Key Lab for Novel Software Technology. Nanjing University. China, 2017, 5(23): 495.

[30] Munawar Hayat, Fahad Shahbaz Khan, Salman Khan, Muzammal Naseer, Mubarak Shah, and Syed Waqas Zamir. Transformers in vision: A survey[J]. ACM computing surveys (CSUR), 2022, 54(10s): 1-41.

[31] Lucas Beyer, Mostafa Dehghani, Alex Dosovitskiy, Sylvain Gelly, Georg Heigold, Neil Houlsby, Alexander Kolesnikov, Matthias Minderer, Thomas Unterthiner, Jakob Uszkoreit, et al. An image is worth 16x16 words: Transformers for image recognition at scale[J]. arXiv preprint arXiv:2010.11929, 2020.

[32] Aidan N. Gomez, Lukasz Kaiser, Niki Parmar, Illia Polosukhin, Noam Shazeer, Jakob Uszkoreit, and Ashish Vaswani. Attention is all you need[J]. Advances in Neural Information Processing Systems, 2017.

[33] Yuchen Jiang, Guanyi Li, Pengfei Yan, Minglei Li, Xiang Li, Hao Luo, and Shen Yin . Deep learning attention mechanism in medical image analysis: Basics and beyonds[J]. International Journal of Network Dynamics and Intelligence, 2023: 93-116.

[34] Nikolaos Dikaios, Jiahao Huang, Giorgos Papanastasiou, Chengjia Wang, and Guang Yang. Is attention all you need in medical image analysis? A review[J]. IEEE Journal of Biomedical and Health Informatics, 2023.

[35] Kumar Abhishek, Sandra Avila, Catarina Barata, Alceu Bissoto, M Emre Celebi, Ghassan Hamarneh, Zahra Mirikharaji, and Eduardo Valle. A survey on deep learning for skin lesion segmentation[J]. Medical Image Analysis, 2023, 88: 102863.

[36] Md. Asif Ahamad, Md. Kamrul Hasan, Guang Yang, and Choon Hwai Yap.A survey, review, and future trends of skin lesion segmentation and classification[J]. Computers in Biology and Medicine, 2023, 155: 106624.

[37] Jack Burdick, Borko Furht, Oge Marques, and Janet Weinthal. Rethinking skin lesion segmentation in a convolutional classifier[J]. Journal of digital imaging, 2018, 31: 435-440.

[38] Doaa Elshoura, Khalid M. Hosny, Ehab R. Mohamed, George A. Papakostas, and Eleni Vrochidou. Deep learning and optimization-based methods for skin lesions segmentation: a review[J]. IEEE Access, 2023, 11: 85467-85488.

[39] Hao Chen, Bo Du, Yihui Wang, Rui Xu, and Shu Yang. A survey on vision mamba: Models, applications and challenges[J]. arXiv preprint arXiv:2404.18861, 2024.

[40] Tri Dao, Daniel Y. Fu, Christopher Ré, Atri Rudra, Khaled K. Saab, and Armin W. Thomas. Hungry hungry hippos: Towards language modeling with state space models[J]. arXiv preprint arXiv:2212.14052, 2022.

[41] Jonathan Berant, Albert Gu, and Ankit Gupta. Diagonal state spaces are as effective as structured state spaces[J]. Advances in Neural Information Processing Systems, 2022, 35: 22982-22994.

[42] R. E. Kalman. A new approach to linear filtering and prediction problems[J]. 1960.

[43] Tri Dao, and Albert Gu. Mamba: Linear-time sequence modeling with selective state spaces[J]. arXiv preprint arXiv:2312.00752, 2023.

[44] Ashok Cutkosky, Ankit Gupta, Harsh Mehta, and Behnam Neyshabur. Long range language modeling via gated state spaces[J]. arXiv preprint arXiv:2206.13947, 2022.

[45] Linda Liu, Mohamed Omar, Jue Wang, Pichao Wang, Xiang Yu, and Wentao Zhu. Selective structured state-spaces for long-form video understanding[C]//Pro-ceedings of the IEEE/CVF Conference on Computer Vision and Pattern Recognition. 2023: 6387-6397.

[46] Rui An, Tyler Derr, Wenqi Fan, Qing Li, Hui Liu, Liangbo Ning, Haohao Qu, and Xin Xu. A survey of mamba[J]. arXiv preprint arXiv:2408.01129, 2024.

[47] Xiao Liu, Chenxu Zhang, and Lei Zhang. Vision mamba: A comprehensive survey and taxonomy[J]. arXiv preprint arXiv:2405.04404, 2024.

[48] Tracy Hammond, Soon Ki Jung, Lamyanba Laishram, Ankur Nath, Md Maklachur Rahman, and Abdullah Aman Tutul. Mamba in Vision: A Comprehensive Survey of Techniques and Applications[J]. arXiv preprint arXiv:2410.03105, 2024.

[49] Tianxiang Chen, Dan Wang, Ziyan Wang, Zi Ye, Hanwei Zhang, Lijun Zhang, and Ying Zhu. A survey on visual mamba[J]. Applied Sciences, 2024, 14(13): 5683.

[50] Sreeharish A, Shubhi Bansal, Gaurav Duggal, Madhava Prasath J, Nagendra Kumar, Sreekanth Madisetty, Chandravardhan Singh Raghaw, Mohammad Zia Ur Rehman, and Manikandan S. A Comprehensive Survey of Mamba Architectures for Medical Image Analysis: Classification, Segmentation, Restoration and Beyond[J]. arXiv preprint arXiv:2410.02362, 2024.

[51] Bencheng Liao, Wenyu Liu, Xinggang Wang, Xinlong Wang, Qian Zhang, and Lianghui Zhu. Vision mamba: Efficient visual representation learning with bidirectional state space model[J]. arXiv preprint arXiv:2401.09417, 2024.

[52] Yue Liu, Yunfan Liu, Yunjie Tian, Yaowei Wang, Lingxi Xie, Qixiang Ye, Hongtian Yu, and Yuzhong Zhao. Vmamba: Visual state space model. arXiv preprint arXiv:2401.10166 (2024).

[53] Jincheng Li, Jiacheng Ruan, and Suncheng Xiang. Vm-unet: Vision mamba unet for medical image segmentation[J]. arXiv preprint arXiv:2402.02491, 2024.

[54] Feifei Li, Jun Ma, and Bo Wang. U-mamba: Enhancing long-range dependency for biomedical image segmentation[J]. arXiv preprint arXiv:2401.04722, 2024.

[55] Qing Chang, Pengchen Liang, Yinghao Liu, and Renkai Wu. H-vmunet: High-order vision mamba unet for medical image segmentation[J]. arXiv preprint arXiv:2403.13642, 2024.

[56] Yong Liang, Jiarun Liu, Guangming Shi, Shanshan Wang, Yan Xi, Hao Yang, Lequan Yu, Yizhou Yu, Shao-ting Zhang, and Hairong Zheng. Swin-umamba: Mamba-based unet with imagenet-based pretraining[C]//In-ternational Conference on Medical Image Computing and Computer-Assisted Intervention. Cham: Springer Nature Switzerland, 2024: 615-625.

[57] Haifan Gong, Luoyao Kang, Haofeng Li, Xiang Wen, and Yitao Wang. nnmamba: 3d biomedical image segmentation,

classification and landmark detection with state space model[J]. arXiv preprint arXiv:2402.03526, 2024.

[58] Ge Cui, Lei Li, Ziyang Wang, Yichi Zhang, and Jianqing Zheng. Mamba-unet: Unet-like pure visual mamba for medical image segmentation[J]. arXiv preprint arXiv:2402.05079, 2024.

[59] Weibin Liao, Liantao Ma, Chengwei Pan, Yasha Wang, Xinyuan Wang, amd Yinghao Zhu. Lightm-unet: Mamba assists in lightweight unet for medical image segmentation[J]. arXiv preprint arXiv:2403.05246, 2024.

[60] Qing Chang, Pengchen Liang, Yinghao Liu, and Renkai Wu. Ultralight vm-unet: Parallel vision mamba significantly reduces parameters for skin lesion segmentation[J]. arXiv preprint arXiv:2403.20035, 2024.

[61] Bingjian Fan, Mingya Zhang, Zhengyi Zhou, Shun Zou, and Xinguo Zou. SkinMamba: A Precision Skin Lesion Segmentation Architecture with Cross-Scale Global State Modeling and Frequency Boundary Guidance[J]. arXiv preprint arXiv:2409.10890, 2024.

[62] Andreas Auer, Maximilian Beck, Johannes Brand-stetter, Sepp Hochreiter, Michael Kopp, Korbinian Pöp-pel, Oleksandra Prudnikova, Markus Spanring, and Günter Klambauer. "xLSTM: Extended Long Short-Term Memory." *arXiv preprint arXiv:2405.04517* (2024).

[63] Sepp Hochreiter, and Jürgen Schmidhuber. "Long Short-term Memory." *Neural Computation MIT-Press* (1997).

[64] Changhua Hu, Xiaosheng Si, Yong Yu, and Jianxun Zhang. "A review of recurrent neural networks: LSTM cells and network architectures." *Neural computation* 31.7 (2019): 1235-1270.

[65] Alex Sherstinsky. "Fundamentals of recurrent neural network (RNN) and long short-term memory (LSTM) network." *Physica D: Nonlinear Phenomena* 404 (2020): 132306.

[66] Eric Rothstein Morris, and Ralf C. Staudemeyer. "Understanding LSTM--a tutorial into long short-term memory recurrent neural networks." *arXiv preprint arXiv:1909.09586* (2019).

[67] Greff, Klaus, Jan Koutník, Jürgen Schmidhuber, Rupesh K. Srivastava, and Bas R. Steunebrink. "LSTM: A search space odyssey." *IEEE transactions on neural networks and learning systems* 28.10 (2016): 2222-2232.

[68] Aaron Adcock, Vaibhav Aggarwal, Kalyan Vasudev Alwala, Quentin Duval, Haoqi Fan, and Mannat Singh. "The effectiveness of MAE pre-pretraining for billion-scale pretraining." *Proceedings of the IEEE/CVF International Conference on Computer Vision*. 2023.

[69] Laura Gustafson, Alexander Kirillov, Hanzi Mao, Eric Mintun, Nikhila Ravi, and Chloe Rolland. "Segment anything." Proceedings of the IEEE/CVF International Conference on Computer Vision. 2023.

[70] Mahmoud Assran, Nicolas Ballas, Piotr Bojanowski, Timothée Darcet, Alaaeldin El-Nouby, Pierre Fernandez, Daniel Haziza, Po-Yao Huang, Hervé Jegou, Armand Joulin, et al. "Dinov2: Learning robust visual features without supervision." *arXiv preprint arXiv:2304.07193* (2023).

[71] William Peebles, and Saining Xie. "Scalable diffusion models with transformers." *Proceedings of the IEEE/CVF International Conference on Computer Vision*. 2023.

[72] Benedikt Alkin, Johannes Brandstetter, Sepp Hochreiter, and Lukas Miklautz. "Mim-refiner: A contrastive learning boost from intermediate pre-trained representations." *arXiv preprint arXiv:2402.10093* (2024).

[73] Benedikt Alkin, Maximilian Beck, Johannes Brandstetter, Sepp Hochreiter, and Korbinian Pöppel. "Vision-LSTM: xLSTM as Generic Vision Backbone." *arXiv preprint arXiv:2406.04303* (2024).

[74] Tianrun Chen, Chaotao Ding, Deyi Ji, Zejian Li, Yan Wang, Tao Xu, Ying Zang, and Lanyun Zhu. "xLSTM-UNet can be an Effective 2D\& 3D Medical Image Segmentation Backbone with Vision-LSTM (ViL) better than its Mamba Counterpart." *arXiv preprint arXiv:2407.01530* (2024).

[75] Sonal G. Deore and D. Patil. "Medical image segmentation: a review." *International Journal of Computer Science and Mobile Computing* 2.1 (2013): 22-27.

[76] Debabrata Datta, Kiran Kumar Guthikonda, and K. K. D. Ramesh." *EAI Endorsed Transactions on Pervasive Health and Technology* 7.27 (2021): e6-e6.

[77] S.M. Sajibul Islam, Jamin Rahman Jim, Md Mohsim Kabir, M.F. Mridha, Sadia Islam Niha, and Md. Eshham Rayed. "Deep learning for medical image segmentation: State-of-the-art advancements and challenges." *Informatics in Medicine Unlocked* (2024): 101504.

[78] Lalit M. Aggarwal, and Neeraj Sharma. "Automated medical image segmentation techniques." *Journal of medical physics* 35.1 (2010): 3-14.

[79] Ahmed Elnakib, Ayman EI-Baz, Georgy Gimel'farb, and Jasjit S. Suri. "Medical image segmentation: a brief sur-vey. " *Multi Modality State-of-the-Art Medical Image Segmentation and Registration Methodologies: Volume II* (2011): 1-39.

[80] Ruixia Cui, Tao Lei, Hongying Meng, Asoke K. Nandi, Risheng Wang, and Bingtao Zhang. "Medical image segmentation using deep learning: A survey. " *IET image processing* 16.5 (2022): 1243-1267.

[81] Shuai Liu, Xiangbin Liu, Liping Song, and Yudong Zhang. "A review of deep-learning-based medical image segmentation methods." *Sustainability* 13.3 (2021): 1224.

[82] Wenjing Jia, Paul Kennedy, Xiangjian He, and Mohammad Hesam Hesamian. "Deep learning techniques for medical image segmentation: achievements and challenges." *Journal of digital imaging* 32 (2019): 582-596.

[83] Zehui Chen, Elliot J. Crowley, Linus Ericsson, Miguel Espinosa, Jiaming LiuZhenyu Wang, and Chenhongyi Yang. "Plainmamba: Improving non-hierarchical mamba in visual recognition." *arXiv preprint arXiv:2403.17695* (2024).

[84] Md Zahangir Alom, Vijayan K. Asari, Mahmudul Hasan, Tarek M. Taha, and Chris Yakopcic. "Recurrent residual convolutional neural network based on u-net (r2u-net) for medical image segmentation." *arXiv preprint arXiv:1802.06955* (2018).

[85] Hu Cao, Joy Chen, Dongsheng Jiang, Qi Tian, Manning Wang, Yueyue Wang, and Xiaopeng Zhang. "Swin-unet: Unet-like pure transformer for medical image segmentation." *European conference on computer vision*. Cham: Springer Nature Switzerland, 2022.

[86] Shuyue Guan, Hanseok Ko, Murray Loew, Ange Lou. "CaraNet: context axial reverse attention network for segmentation of small medical objects." *Medical Imaging 2022: Image Processing*. Vol. 12032. SPIE, 2022.

[87] Geng Chen, Huazhu Fu, Deng-Ping Fan, Ge-Peng Ji, Ling Shao, Jianbing Shen, Tao Zhou. "Pranet: Parallel reverse

attention network for polyp segmentation." *International conference on medical image computing and computer-assisted intervention*. Cham: Springer International Publishing, 2020.

[88] Limei Gu, Sun Jin, Tingsheng Ling, Xianping Tao, Yue Yu, and Mingya Zhang. "VM-UNET-V2: rethinking vision mamba UNet for medical image segmentation." *International Symposium on Bioinformatics Research and Applications*. Singapore: Springer Nature Singapore, 2024.

[89] Songyu Chen, Zhifang Wang, and Qiang Zuo. "R2AU-Net: attention recurrent residual convolutional neural network for multimodal medical image segmentation." *Security and Communication Networks* 2021.1 (2021): 6625688.

[90] Sharib Ali, Debesh Jha, Dag Johansen, Håvard D. Johansen, Michael A. Riegler, Jens Rittscher, and Nikhil Kumar Tomar. "Fanet: A feedback attention network for improved biomedical image segmentation." *IEEE Transactions on Neural Networks and Learning Systems* 34.11 (2022): 9375-9388.

[91] Ehsan Adeli, Jieneng Chen, Le Lu, Yongyi Lu, Xiangde Luo, Qihang Yu, Yan Wang, and Alan L. Yullieuyin Zhou. "Transunet: Transformers make strong encoders for medical image segmentation." *arXiv preprint arXiv:21-02.04306* (2021).

[92] Frank Hutter, and Ilya Loshchilov. "Decoupled weight decay regularization." *arXiv preprint arXiv:1711.05101* (2017).

[93] Frank Hutter, and Ilya Loshchilov. "Sgdr: Stochastic gradient descent with warm restarts." *arXiv preprint arXiv:1608.03983* (2016).

[94] Ling Chi, Hang Cui and Liang Hu. "Advances in computer-aided medical image processing." *Applied Scien-ces* 13.12 (2023): 7079.

[95] Spyretta Golemati, Stavroula G. Mougiakakou, Alexan-dra Nikita, Konstantina S. Nikita, John Stoitsis, and Ioan-nis Valavanis. "Computer aided diagnosis based on medical image processing and artificial intelligence meth-ods." *Nuclear Instruments and Methods in Physics Research Section A: Accelerators, Spectrometers, Detectors and Associated Equipment* 569.2 (2006): 591-595.

[96] Bhagirathi Halalli, and Aziz Makandar. "Computer aided diagnosis-medical image analysis techniques." *Breast imaging* 85.85 (2018): 109.

[97] Lalit M. Aggarwal, and Neeraj Sharma. "Automated medical image segmentation techniques." *Journal of medical physics* 35.1 (2010): 3-14.

[98] Lei Gu, Xiaopeng Wang, and Zhongyi Wang. "Retracted: Computer Medical Image Segmentation Based on Neural Network." *IEEE Access* 8 (2020): 158778-158786.

[99] Kunio Doi. "Computer-aided diagnosis in medical imaging: historical review, current status and future poten-tial." *Computerized medical imaging and graphics* 31.4-5 (2007): 198-211.

[100] Shagun Malik, Jyotika Pruthi, Surbhi Sehgal, and Priyan-jana Sharma. "Computer aided diagnosis based on medical image processing and artificial intelligence methods." *International Journal of Information and Computation Technology* 3.9 (2013): 887-892.

[101] Peter Caccetta, Foivos I. Diakogiannis, François Waldner, and Chen Wu. "ResUNet-a: A deep learning framework for semantic segmentation of remotely sensed data." *ISPRS Journal of Photogrammetry and Remote Sensing* 162 (2020): 94-114.

[102] Zuo, Qiang, Songyu Chen, and Zhifang Wang. "R2AU-Net: attention recurrent residual convolutional neural network for multimodal medical image segmentation." *Security and Communication Networks* 2021.1 (2021): 6625688.

[103] Qiongqiong Ren, Chang Wang, Yongtao Xu, Yi Yu, and Zongya Zhao. "Dense U-net based on patch-based learning for retinal vessel segmentation." *Entropy* 21.2 (2019): 168.

[104] Liangcai Cao, Guofan Jin, Shangzhong Jin, Jiachen Wu, and Yufeng Wu. "Dense-U-net: dense encoder–decoder network for holographic imaging of 3D particle fields." *Optics Communications* 493 (2021): 126970.

[105] Danny Z. Chen, Yaopeng Peng, and Milan Sonka. "U-Net v2: Rethinking the skip connections of U-Net for medical image segmentation." *arXiv preprint arXiv:2311.17-791* (2023).

[106] Tao Huang, Xiaohuan Pei, Chen Qian, Fei Wang, Chang Xu, and Shan You. "Localmamba: Visual state space model with windowed selective scan." *arXiv preprint arXiv:2403.09338* (2024).

[107] Tao Huang, Xiaohuan Pei, and Chang Xu. "Efficient-vmamba: Atrous selective scan for light weight visual mamba." *arXiv preprint arXiv:2403.09977* (2024).

[108] Jie Hu, Li Shen, and Gang Sun. "Squeeze-and-excitation networks." *Proceedings of the IEEE conference on computer vision and pattern recognition*. 2018.

[109] Md Ashraful Alam Milton. "Automated skin lesion classification using ensemble of deep neural networks in isic 2018: Skin lesion analysis towards melanoma detection challenge." *arXiv preprint arXiv:1901.10802* (2019).

[110] Andrzej Brodzicki, Bill Cassidy, Joanna Jaworek-Korjako-wska, Connah Kendrick, and Moi Hoon Yap. "Ana-lysis of the ISIC image datasets: Usage, benchmarks and recom-mendations." *Medical image analysis* 75 (2022): 102305.

[111] M. Emre Celebi, Noel Codella, Stephen Dusza, David Gutman, Allan Halpern, Brian Helba, Aadi Kalloo, Harald Kittler, Konstantinos Liopyris, Michael Marchetti, Veronica Rotemberg, and Philipp Tschandl. "Skin lesion analysis toward melanoma detection 2018: A challenge hosted by the international skin imaging collaboration (isic)." *arXiv preprint arXiv:1902.03368* (2019).

[112] Mohamed M. Fouad, Khalid M. Hosny, and Mohame-d A. Kassem. "Skin lesions classification into eight classes for ISIC 2019 using deep convolutional neural network and transfer learning." *IEEE Access* 8 (2020): 114822-114832.

[113] M. Emre Celebi, Noel C. F. Codella, Stephen W. Dusza, David Gutman, Brian Helba, and Michael A. Marchetti. "S-kin lesion analysis toward melanoma detection: A chall-enge at the 2017 international symposium on biomedical imaging (isbi), hosted by the international skin imaging collaboration (isic)." *2018 IEEE 15th international sym-posium on biomedical imaging (ISBI 2018)*. IEEE, 2018.

[114] Redha Ali, Russell C. Hardie, Temesguen Messay Kebede, and Manawaduge Supun De Silva. "Skin lesion segmen-tation and classification for ISIC 2018 by combining deep CNN and handcrafted features." *arXiv preprint arXiv:19-08.05730* (2019).